

# La(Sr,Pb)MnO<sub>3</sub> Thin Films through Solution Techniques

I. Maurin, P. Barboux,\* Y. Lassailly, and J. P. Boilot

Laboratoire de Physique de la Matière Condensée, Ecole Polytechnique,  
91128 Palaiseau, France

Received October 7, 1997. Revised Manuscript Received April 15, 1998

Thin films of (La<sub>0.9</sub>Sr<sub>0.1</sub>)MnO<sub>3</sub> have been deposited using a citrate–ethylene glycol method. Si (100) substrates yield polycrystalline films, whereas MgO (100) substrates favor the nucleation of textured films. However, the rough calcination of organics results in a granular morphology with insulating grain boundaries. Sintering can be strongly enhanced by addition of small amounts of lead oxide. When substituted for strontium, lead does not drastically affect the physical properties of the perovskite phase, but allows the formation of a percolative conduction path. Conductive films have been obtained through heat-treatment at temperatures as low as 600 °C. They show a magnetoresistance effect ( $\Delta\rho/\rho_0$ ) of 65% at 175 K in fields up to 8 T.

## Introduction

Giant magnetoresistance effects (GMR) have recently been reported in manganites R<sub>1-x</sub>A<sub>x</sub>MnO<sub>3</sub>, where R and A are rare-earth and alkaline-earth elements respectively.<sup>1</sup> This has opened up the possibility of their use as reading heads for magnetic memories and as magnetic sensors. (La,Sr)MnO<sub>3</sub> compounds are also promising cathodes in solid oxide fuel cells (SOFCs)<sup>2</sup> and catalysts in the oxidation of hydrocarbons or carbon monoxide.<sup>3</sup> Indeed, they reveal electrocatalytic properties toward the reduction of oxygen and a high mobility of oxygen ions in the structure.

Most of these technological applications depend on the electronic conductivity of these materials. Stoichiometric LaMnO<sub>3</sub>, which has a perovskite related structure, is an antiferromagnetic insulator. Partial substitution for trivalent La(III) by divalent M(II) (M = Ca, Sr, Ba, Pb) turns this compound into a ferromagnet. The electrical behavior then switches from a high-temperature semiconductor type to a low-temperature metal-like type at the vicinity of the Curie temperature. In the case of La<sub>1-x</sub>Sr<sub>x</sub>MnO<sub>3</sub>, the composition  $x = 0.1$  is the borderline between the compounds that remain insulating over the whole temperature range and those that undergo a metal–insulator transition. These magnetic and electronic transitions are supposed to result from a mixed valence state Mn<sup>3+</sup>–Mn<sup>4+</sup> that leads to mobile charge carriers and induces the canting of Mn spins (double exchange theory).<sup>4,5</sup>

The manganese oxidation state and the metal–insulator transitions are also changed by nonstoichiometry.<sup>6</sup> Low-temperature synthesis allows a larger oxidation state of manganese associated with the simultaneous presence of cationic vacancies in La and Mn

sites of the perovskite structure: (La,Sr)<sub>1-y</sub>Mn<sub>1-y</sub>O<sub>3</sub>. For example, solution synthesis allows the low-temperature crystallization of a LaMnO<sub>3</sub> ceramic with a metallic behavior without Sr doping.<sup>7</sup>

Most of the expected applications of these materials require thin films (magnetic recording heads) or thick films (oxygen membranes in SOFCs). Cheap and versatile alternatives to physical methods based on evaporation would be the solution techniques. Such methods are particularly suitable for large-scale production or large area coatings. Sol–gel methods based on chelating solvents such as 2-methoxyethanol have already allowed the synthesis of films with a very strong epitaxial character.<sup>8</sup> Methods based on polycarboxylates such as polyacrylates or polymethacrylates have also been reported.<sup>9</sup> Most of the time, a drawback of such deposition processes is that the rheology of the solutions (or their allowed metal concentration) requires repeated coating sequences and intermediate calcinations to obtain films with a thickness still lower than 100 nm. Moreover, the very exothermic calcination of organics results in porous films with insulating character, as will be shown below. Therefore, we here describe a method derived from the Pechini process<sup>10</sup> that we have adapted to the deposition of thicker films by spin-coating. We have investigated the low-temperature crystallization and densification of such films on different substrates in relation with their physical properties. We focused on the La<sub>0.9</sub>Sr<sub>0.1</sub>MnO<sub>3</sub> composition, which is particularly sensitive to the nonstoichiometry, the amount of doping, and the nature of the dopant.

## Experimental Section

(La<sub>1-x</sub>Sr<sub>x</sub>)MnO<sub>3</sub> (with  $x = 0.1$ ) films with a 1 μm thickness have been synthesized using a method derived

(1) McCormack, M.; Jin, S.; Tiefel, T. H.; Fleming, R.M.; Phillips J. M. *Appl. Phys. Lett.* **1994**, *64*, 3045.

(2) Kertesz, M.; Riess, I.; Tanhauser, D. S.; Langpape, R.; Rohr, F. *J. Solid State Chem.* **1982**, *42*, 125.

(3) Petrolekas, P. D.; Metcalfe, I. S. *J. Catal.* **1995**, *152*, 147.

(4) Jonker, G. H. *Physica* **1956**, *22*, 707.

(5) Zener, C. *Phys. Rev.* **1951**, *82*, 403.

(6) Rao, C. N. R.; Cheetham, A. K. *Science* **1996**, *272*, 369.

(7) Verelst M.; Rangavittal N.; Rao, C. N. R.; Rousset A. *J. Solid State Chem.* **1993**, *104*, 74.

(8) Bae, S.-Y.; Wang, S. X. *Appl. Phys. Lett.* **1996**, *69*, 121.

(9) Taguchi, H.; Sugita, A.; Nagao, A. *J. Solid State Chem.* **1996**, *121*, 495.

(10) Pechini, M. P. U.S. Patent 3 330 697, 1967.

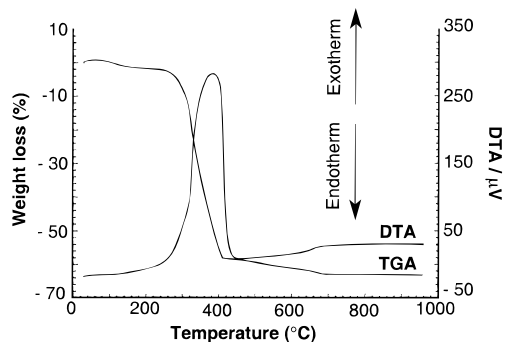


**Figure 1.** TGA–DTA curves of a resin with formal composition  $\text{LaMnO}_3$  (experiments performed at  $10^\circ\text{C}/\text{min}$  under an oxygen flow).

from the citrate–ethylene glycol process. This method has already been applied to the synthesis of ceramics of this perovskite system.<sup>7,11</sup>

$\text{La}(\text{NO}_3)_3 \cdot 6\text{H}_2\text{O}$ ,  $\text{Mn}(\text{NO}_3)_2 \cdot 6\text{H}_2\text{O}$ , and  $\text{Sr}(\text{NO}_3)_2$  were dissolved in water in the appropriate ratio (0.5 M in Mn). A 100 mL portion of this solution was then added to 300 mL of a solution containing citric acid (50 g) and ethylene glycol (12.5 mL), and the mixture was heated to its boiling point until the Mn concentration reached 0.35 M. The viscosity increased during esterification, but as this solution (called A) did not wet the different substrates [ $\text{MgO}$  (100),  $\text{Si}$  (100)], it was not directly adapted to spin-coating.

Therefore, another polymeric solution (called B) was formed by reaction of 25 g of acetylacetone with 35 g of hexamethylenetetramine (HMTA) in acetic acid (ratio acac/HMTA = 1, concentration of acac in acetic acid = 2.9 M).<sup>12</sup> This solution was added to the Pechini solution A in the 1/1 volume ratio. Films were deposited by spin-coating (3500 rpm, 30 s) onto the different substrates. Each coating step deposits around 170 nm of perovskite film. The spin-coating sequence was repeated six times with intermediate pyrolysis at  $400^\circ\text{C}$  for 10 min. Finally, the films were fired in air between 600 and  $1000^\circ\text{C}$  for 12 h. The average thickness of the crystallized films is  $1\ \mu\text{m}$ .

Structure and orientation of the films were characterized by X-ray diffraction in the Bragg–Brentano geometry using  $\text{Cu K}\alpha$  radiation. The indexations are given in the hexagonal system. The morphology of the coatings was observed by scanning electron microscopy. Electrical resistivity measurements have been performed in the temperature range 4–300 K using a four-probe technique.

## Results and Discussion

Drying the solutions derived from this process yields a dark brown resin. Its calcination leads to a large exothermic 60% weight loss around  $350^\circ\text{C}$ , as shown by thermal analysis (Figure 1). In the TGA, residual carbonates are removed at  $700^\circ\text{C}$  just before the crystallization. But, under static conditions, the amorphous black powder obtained after the decomposition of organics crystallizes within a few hours at  $650^\circ\text{C}$ . The films obtained by our deposition process can even

crystallize at lower temperatures ( $550^\circ\text{C}$  for 12 h) when deposited onto  $\text{MgO}$ . The composition of the films has been checked by Rutherford backscattering spectrometry (RBS). The ratio  $\text{La}/\text{Sr}/\text{Mn}$  obtained by simulation of the RBS spectra using the RUMP program<sup>13</sup> is in good agreement with the composition of the starting solution.

The X-ray diffraction patterns of films deposited onto the two different substrates are shown in Figure 2. They have been indexed in the rhombohedral symmetry ( $R\bar{3}c$  space group). After deposition of a single layer, the films grown onto  $\text{Si}$  (100) are polycrystalline, whereas they appear strongly textured when deposited onto  $\text{MgO}$  (100) and exhibit strong harmonics along the (102) direction (Figure 2a,b). This direction corresponds to the (001) direction of the undistorted cubic perovskite structure and the texturing effect can be explained by the well-known coherence of the oxygen packings along the (001) directions of both the perovskite structure and the  $\text{MgO}$  rocksalt structure. However, because of the large lattice mismatch ( $\text{MgO}$ ,  $4.2\ \text{\AA}$ ;  $\text{LaMnO}_3$ ,  $3.9\ \text{\AA}$  in the pseudocubic cell), the texturing effect is weak. Indeed, the rocking curves indicate only a very broad distribution of the directions around the (204) line (in terms of full-width at half-maximum:  $\text{fwhm} = 4.6^\circ$  for a film fired at  $550^\circ\text{C}$ , inset of Figure 2b). This distribution is enlarged by the Mn concentration in the stock solution. The texturing effect becomes weaker in the thicker films (six layers deposited). Then, some crystallites are oriented along different directions, as evidenced by the peaks at  $2\theta \sim 32.7^\circ$ , corresponding to the (110) and (104) lines (Figure 2c). The crystallization mechanism of the perovskite phase has already been investigated and is probably nucleation-controlled.<sup>14</sup> As the temperature of crystallization is lowered from  $650$  to  $550^\circ\text{C}$  by deposition onto  $\text{MgO}$ , we believe that the substrate induces the nucleation and orientates the growth of the crystalline phase.

One should comment on the apparently poor texturing of these films (rocking curve of  $4.6^\circ$  obtained onto  $\text{MgO}$ ) as compared to the epitaxial character of films deposited by other solution methods such as sol–gel<sup>8</sup> or by nebulized spray pyrolysis<sup>15</sup> (rocking curve  $0.15^\circ$  onto  $\text{SrTiO}_3$  or  $\text{LaAlO}_3$ ). It is well-known that the film texturing is a competition between the interaction energy with the substrate and the bulk internal stresses due to the volume changes during the calcination and the crystallization. Therefore, larger texturing is observed when the substrate interaction is more favorable ( $\text{SrTiO}_3$  is better than  $\text{MgO}$  for a perovskite growth) and for the thinner films. Better texturing is also obtained when the crystallization occurs in situ during the deposition (pulse laser deposition, nebulized spray pyrolysis) as opposed to those methods that require a postdeposition annealing of the film. This is a general drawback of solution processes such as our Pechini method.

The very exothermic decomposition of organics observed in the thermal analysis is also a drawback for the synthesis of dense and conductive films. Indeed,

(13) Doolittle, L. R. *Nucl. Instrum. Methods B* **1985**, *9*, 344.

(14) Maurin, I.; Barboux, P.; Boilot, J. P. *Material Research Symposium Series*; 1997; Vol. 453, p 41.

(15) Aiyer, H. N.; Raju, A. R.; Subbanne, G. N.; Rao, C. N. R. *Chem. Mater.* **1997**, *9*, 755.

(11) Van Roosmalen, J. A. M.; Cordfunke, E. H. P.; Huijsmans, J. P. P. *Solid State Ionics* **1993**, *66*, 285.

(12) Valente, I. Thesis of the University P. et M. Curie, **1989**.

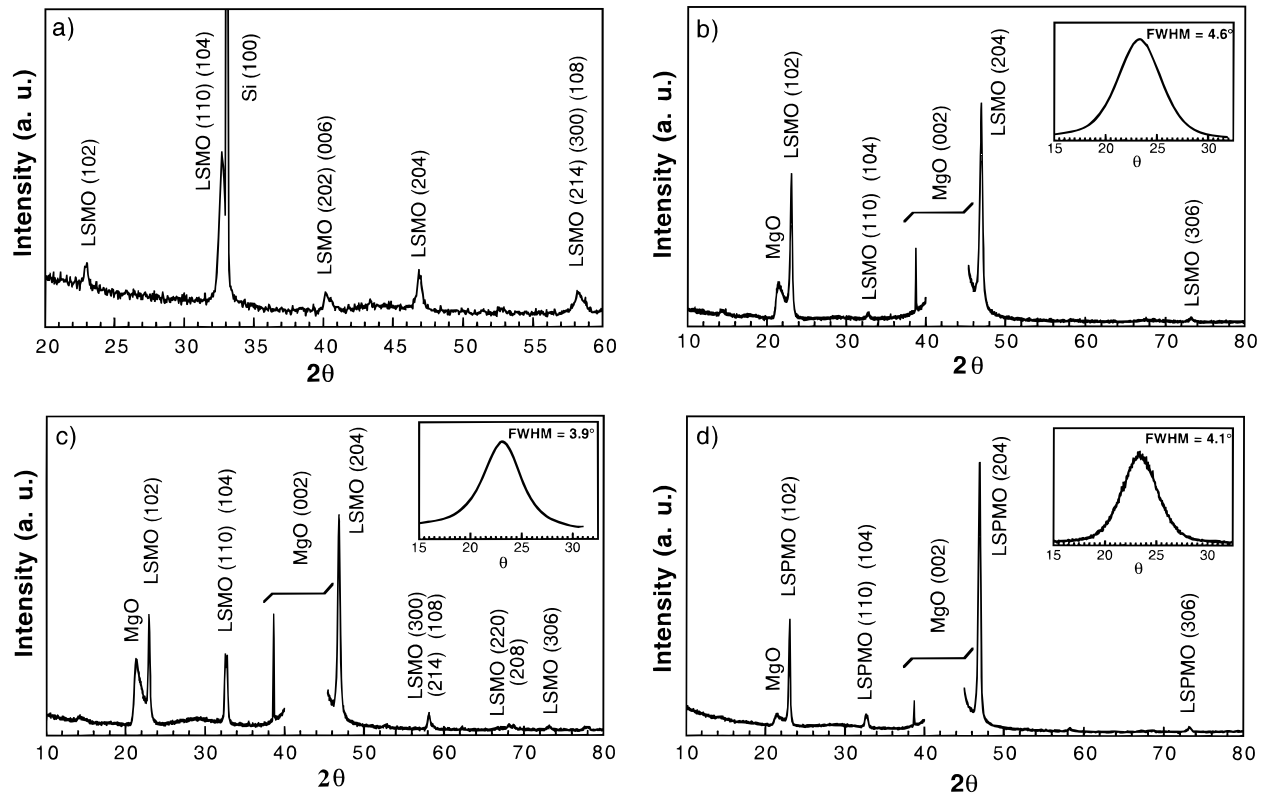


**Figure 2.** XRD pattern of (a) La<sub>0.9</sub>Sr<sub>0.1</sub>MnO<sub>3</sub> film (a single layer deposited) on Si (100) heat-treated at 650 °C for 12 h; (b) La<sub>0.9</sub>Sr<sub>0.1</sub>MnO<sub>3</sub> film (a single layer deposited) onto MgO (100) heat-treated at 550 °C for 12 h; (c) La<sub>0.9</sub>Sr<sub>0.1</sub>MnO<sub>3</sub> film (six layers deposited) onto MgO, heat-treated at 550 °C for 12 h; (d) La<sub>0.9</sub>Sr<sub>0.075</sub>Pb<sub>0.025</sub>MnO<sub>3</sub> film (six layers deposited) onto MgO, heat-treated at 550 °C for 12 h.

all the films of the (La,Sr)MnO<sub>3</sub> system heat-treated from 550 to 950 °C are insulating at room temperature. When observed by scanning electron microscopy, a film fired at 650 °C appears very porous and consists of weakly connected grains with an average grain size of 30 nm (Figure 3a). This grain morphology may be driven by the rough calcination steps yielding a burst into small grains. After heating at higher temperature (950 °C), grain coarsening occurs, but the films remain porous (Figure 3b).

To overcome this drawback and to obtain a better sintering of the films, we have added an oxide forming a liquid phase during the crystallization process. Lead oxide has a melting point of 890 °C and forms with small amounts of La<sub>2</sub>O<sub>3</sub> an eutectic at 770 °C.<sup>16</sup> Moreover, as Pb can enter the perovskite phase in substitution for La,<sup>17</sup> two methods of lead addition have been investigated. In the first method, lead has been added in substitution for lanthanum. This corresponds to the formal La<sub>0.9</sub>Sr<sub>0.1-y</sub>Pb<sub>y</sub>MnO<sub>3</sub> composition. In the second method, PbO has been added in excess of the perovskite stoichiometry corresponding to the composition La<sub>0.9</sub>Sr<sub>0.1</sub>MnO<sub>3</sub>, *y*PbO. In this latter case, as PbO is highly volatile, it may be eliminated afterward by firing at temperatures above 900 °C. In both cases, lead nitrate has been added to the Pechini solution in the ratio Pb/Mn = 0.025. After heat treatment at 550 °C, the films are crystallized and a texturing effect larger than for lead-free samples is observed by X-ray diffraction (Figure 2d). When observed by SEM, they exhibit an

average grain size of 30 nm (Figure 3c) similar to that of the lead-free samples (Figure 3a), but the films are more uniform. Grain growth occurs at higher temperatures and the particle size increases to 200 nm at 800 °C and then to 300 nm at 950 °C (Figure 3d). This grain size is larger than that obtained for the lead-free samples (Figure 3b), and the grain boundaries are characteristic of the occurrence of a molten phase. The films are still porous, but the grains are well connected to each other. Samples prepared following either of the two methods of lead addition do not present any difference in the microstructure. As a conclusion, densification is optimal at low temperature (600–700 °C), whereas, at higher temperatures, the connectivity between grains is weaker but still above the percolation threshold. Indeed, all the lead-containing films are conductive after heat treatment between 600 and 950 °C.

To have a clear understanding of the effect of lead, we first discuss the physical properties of ceramics. We have studied three powders with the compositions La<sub>0.9</sub>Sr<sub>0.1</sub>MnO<sub>3</sub>, La<sub>0.9</sub>(Sr<sub>0.075</sub>Pb<sub>0.025</sub>)MnO<sub>3</sub>, and La<sub>0.9</sub>Sr<sub>0.1</sub>MnO<sub>3</sub>, 0.025PbO. The powders, obtained from our dried solutions and calcined at 600 °C, have been pressed into pellets and sintered for 12 h at 850 °C, so that lead has not evaporated. However, the lead content is too small to affect the cell parameters and to be detected by X-ray diffraction.

The resistivity of the ceramics has been measured on bar-shaped samples (1.5 × 2 × 5 mm<sup>3</sup>) (Figure 4). The temperature dependence of the resistivity exhibits a broad peak, the maximum of which is associated with

(16) Cassedanne, J. *Ann. Acad. Brasil. Cienc.* **1964**, *36*, 414.

(17) Searle, C. W.; Wang, S. T. *Can. J. Phys.* **1970**, *48*, 2023.

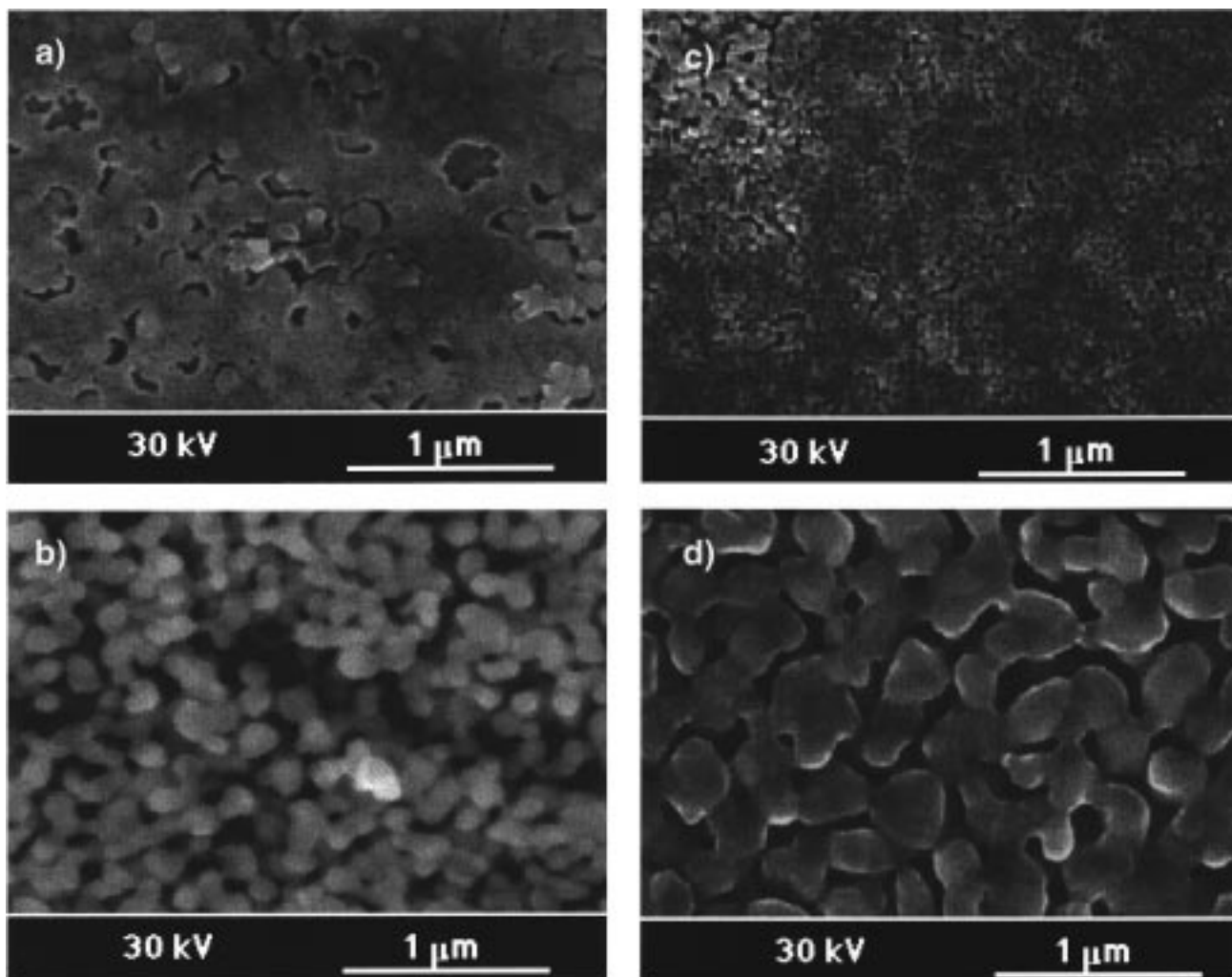


**Figure 3.** Scanning electron microscopy of thin films deposited onto MgO (100): (a)  $\text{La}_{0.9}\text{Sr}_{0.1}\text{MnO}_3$  heat-treated at 650 °C for 12 h, (b) same film heat-treated at 950 °C for 2 h, (c)  $\text{La}_{0.9}\text{Sr}_{0.075}\text{Pb}_{0.025}\text{MnO}_3$  heat-treated at 650 °C for 12 h, (d) same film heat-treated at 950 °C for 2 h.

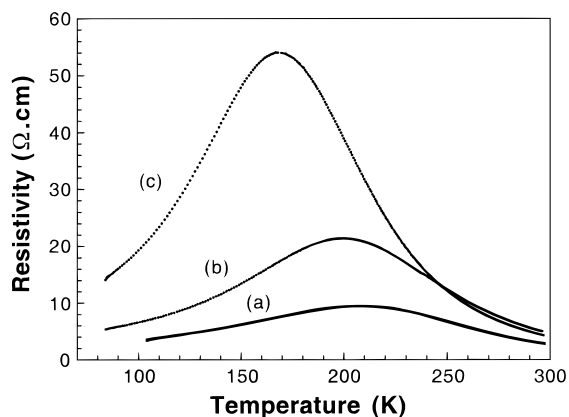


**Figure 4.** Electrical resistivities of ceramics sintered at 850 °C for 12 h: (a)  $\text{La}_{0.9}\text{Sr}_{0.1}\text{MnO}_3$ , (b)  $\text{La}_{0.9}\text{Sr}_{0.075}\text{Pb}_{0.025}\text{MnO}_3$ , (c)  $\text{La}_{0.9}\text{Sr}_{0.1}\text{MnO}_3, 0.025\text{PbO}$ .

the transition from a semiconducting regime at high temperature to a metallic behavior at low temperature. Such a metal–insulator transition is only observed, at this low level of La substitution, in the case of ceramics densified below 1000 °C.<sup>18</sup> In this case, large amounts

of cationic vacancies increase the manganese oxidation state. Indeed, we have measured a  $\text{Mn}^{4+}$  content of 38% in all our ceramics by iodometric titration.

The bulk samples of  $\text{La}_{0.9}\text{Sr}_{0.1}\text{MnO}_3$  and  $\text{La}_{0.9}(\text{Sr}_{0.075}\text{Pb}_{0.025})\text{MnO}_3$  compositions both show a transition at 200 K. Therefore, small amounts of lead do not affect the physical properties when substituted for strontium. This result may be surprising as the substitution for La by Pb alone ( $\text{La}_{1-x}\text{Pb}_x\text{MnO}_3$  compounds) shifts the metal–insulator transition above room temperature.<sup>19</sup> This transition is observed above 300 K for  $\text{La}_{0.9}\text{Pb}_{0.1}\text{MnO}_3$  and around 150 K for  $\text{La}_{0.9}\text{Sr}_{0.1}\text{MnO}_3$ . One should therefore expect an increase of the transition temperature ( $T_p$ ) upon the replacement of some Sr by Pb. However, the disorder associated to the distribution of too many different species in the La site (La, Sr, Pb, and the vacancies introduced by the low-temperature synthesis) may cause larger strain fields and a downshift of  $T_p$ , as discussed by Rodriguez et al.<sup>20</sup>

On the other hand, lead in excess produces a shift of the transition down to 170 K in the case of the

(18) Mahesh, R.; Mahendiran, R.; Raychaudhuri, A. K.; Rao, C. N. R. *J. Solid State Chem.* **1995**, *114*, 297.

(19) Mahendiran, R.; Mahesh, R.; Raychaudhuri, A. K.; Rao, C. N. R. *J. Phys. D, Appl. Phys.* **1995**, *28*, 1743.

(20) Rodríguez-Martínez, L. M.; Attfield, J. P. *Phys. Rev. B* **1996**, *54*, 15 624.

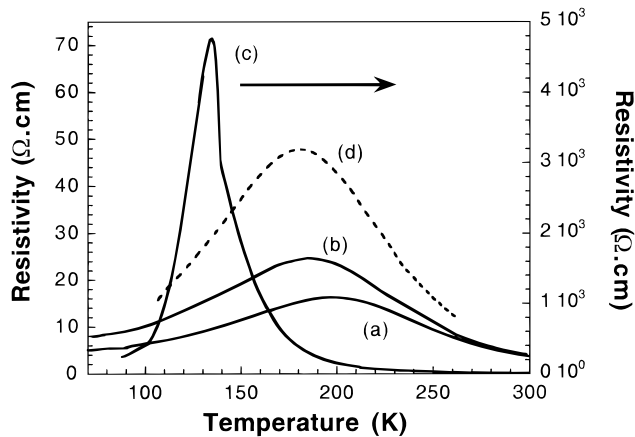


**Figure 5.** Electrical resistivities of (a) La<sub>0.9</sub>Sr<sub>0.075</sub>Pb<sub>0.025</sub>MnO<sub>3</sub> film (650 °C, 12 h); (b) La<sub>0.9</sub>Sr<sub>0.1</sub>MnO<sub>3</sub>, 0.025PbO film (650 °C, 12 h); (c) La<sub>0.9</sub>Sr<sub>0.1</sub>MnO<sub>3</sub>, 0.025PbO film (950 °C, 2 h) (d) La<sub>0.9</sub>-Sr<sub>0.1</sub>MnO<sub>3</sub>, 0.025PbO ceramic (950 °C, 2 h).

La<sub>0.9</sub>Sr<sub>0.1</sub>MnO<sub>3</sub>, 0.025PbO sample. The perovskite solid solution ABO<sub>3</sub> accepts a wide range of nonstoichiometry for the A/B ratio in this LaMnO<sub>3</sub> compound.<sup>21</sup> Therefore, lead has probably entered the structure in the A site as a substituent for La. Since it has been introduced in excess, the chemical formula La<sub>0.9/1.025</sub>Sr<sub>0.1/1.025</sub>Pb<sub>0.025/1.025</sub>Mn<sub>1/1.025</sub>V<sub>0.025/1.025</sub>O<sub>3</sub>, where V denotes a vacancy in the B site, is more appropriate to describe the nominal composition. Recent works have shown that vacancies in the manganese site are detrimental to the conductivity and lower the temperature of the insulator to metal transition.<sup>22,23</sup>

The films synthesized at 650 °C (six layers deposited) all exhibit a metal–insulator transition like the corresponding ceramics (Figure 5). The behavior of the film with the La<sub>0.9</sub>(Sr<sub>0.075</sub>Pb<sub>0.025</sub>)MnO<sub>3</sub> composition is strictly similar to that of the ceramic heat-treated at 850 °C with a transition temperature around 200 K (Figure 5a). However, the film with extra lead (La<sub>0.9</sub>Sr<sub>0.1</sub>MnO<sub>3</sub>, 0.025PbO) has a transition temperature (190 K) slightly higher than the corresponding ceramic (170 K). This difference may be associated with a different balance of the vacancy concentration in the A and B sites because of the different synthesis temperatures (650 °C for the film and 850 °C for the ceramic). But, since this difference of  $T_p$  is not observed for the film and the ceramic with lead substituted for Sr (Figure 4b and 5a), we propose another hypothesis. At the lower temperatures (650 °C), a perovskite may form with the ratio A/B = 1. Some Sr (probably less reactive than Pb) has not entered the structure and we have obtained La<sub>0.9</sub>-Sr<sub>0.075</sub>Pb<sub>0.025</sub>MnO<sub>3</sub>, 0.025SrO (or SrCO<sub>3</sub>). Then, the composition in the perovskite cell of both films is the same: La<sub>0.9</sub>Sr<sub>0.075</sub>Pb<sub>0.025</sub>MnO<sub>3</sub>. Therefore,  $T_p$  is similar, but the resistivity is higher in the films with lead in excess because of impurities (SrO or SrCO<sub>3</sub>) at the grain boundaries. Between 650 and 850 °C, it is obvious from the change in the morphology of the films that some liquid phase appears. This allows the strontium to

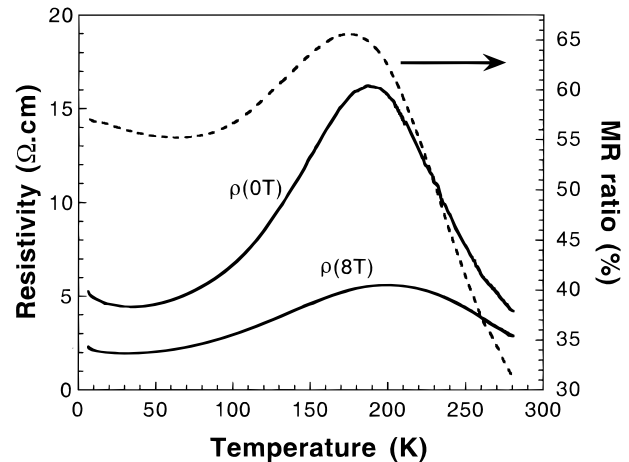


**Figure 6.** Electrical resistivities under different magnetic fields and magnetoresistive ratio ( $\Delta\rho/\rho_0$ ) of a La<sub>0.9</sub>Sr<sub>0.075</sub>Pb<sub>0.025</sub>MnO<sub>3</sub> thin film heat-treated at 650 °C, 12 h.

enter the perovskite phase, forming manganese vacancies that shift down  $T_p$  in the ceramic.

Note that the RBS analysis indicates no loss of lead in the films synthesized at 650 °C. On the contrary, 50% of the lead has evaporated from the La<sub>0.9</sub>Sr<sub>0.1</sub>MnO<sub>3</sub>, 0.025PbO film heat-treated at 950 °C for 2 h. Also, the resistivity increases by 2 orders of magnitude as compared to the same film heat-treated at 650 °C only (Figure 5b,c). This is in good agreement with the lower densification observed by SEM. But, a drastic decrease of the metal–insulator transition temperature is also observed. This might be associated to the microstructural change. But, Mahesh et al.<sup>24</sup> have demonstrated that grain growth increases the transition temperature, whereas we observe that the larger grains (950 °C) yield the lower  $T_p$ . Moreover, the corresponding ceramic heat-treated under the same conditions does not exhibit such a large shift both in the transition temperature and in the resistivity value (Figure 5d). Therefore, the decrease of  $T_p$  is better explained by an interdiffusion with the MgO substrate<sup>25</sup> after heat-treatment at 950 °C. However, it is difficult to verify this interdiffusion by RBS because of the granular aspect of the films.

Figure 6 shows the temperature variation of resistivity of a La<sub>0.9</sub>(Sr<sub>0.075</sub>Pb<sub>0.025</sub>)MnO<sub>3</sub> film measured upon warming in 0 and 8 T magnetic fields. The film was deposited onto MgO (001) and heat-treated at 650 °C for 12 h. The application of a magnetic field strongly reduces the resistivity. The magnetoresistance ratio, MR, defined here as  $(\rho(H=0T) - \rho(H=8T))/\rho(H=0T)$ , is 65% at 180 K. The MR still rising at low temperatures is attributed to spin-dependent scattering or tunneling at grain boundaries.<sup>26–28</sup> Indeed, such a low-field MR component has only been observed in polycrystalline thin films or ceramics.

(24) Mahesh, R.; Mahendiran, R.; Raychaudhuri, A. K.; Rao, C. N. R. *Appl. Phys. Lett.* **1996**, *68*, 2291.

(25) Anane, J.; Dupas, C.; Le Dang, K.; Renard, J. P.; Veillet, P.; Pinsard, L.; Revcolevschi, A. *Appl. Phys. Lett.* **1996**, *69*, 1160.

(26) Mathur, N. D.; Burnell, G.; Isaac, S. P.; Jackson, T. J.; Teo, B.-S.; MacManus-Driscoll, J. L.; Cohen, L. F.; Evetts, J. E.; Blamire, M. G. *Nature* **1997**, *387*, 266.

(27) Gupta, A.; Gong, G. Q.; Gang Xia, Duncombe, P. R.; Lecoeur, P.; Trouilloud, P.; Wang, Y. Y.; Dravid, V. P.; Sun, J. Z. *Phys. Rev. B* **1996**, *54*, R15 629.

(28) Hwang, H. Y.; Cheong, s.-W.; Ong, N. P.; Batlogg, B. *Phys. Rev. Lett.* **1996**, *77*, 2041.

(21) van Roosmalen, J. A. M.; van Vlaanderen, P.; Cordfunke, E. H. P.; Ijdo, W. L.; Ijdo, D. J. W. *J. Solid State Chem.* **1995**, *117*, 420.

(22) Arulraj, A.; Mahesh, R.; Subbanna, G. N.; Mahendiran, R.; Raychaudhuri, A. K.; Rao, C. N. R. *J. Solid State Chem.* **1996**, *127*, 87.

(23) Töpfer, J.; Goodenough, J. B. *Chem. Mater.* **1997**, *9*, 1467.

### Conclusion

We have used a simple and versatile solution process to deposit (La,Sr)MnO<sub>3</sub> thin films onto various substrates. In such methods, the exothermic decomposition of organics yields porous films. Therefore, we describe the effect of the addition of slight amounts of a phase with a low melting point (PbO) that allows a better particle connectivity. Lead added as a substituent for Sr does not strongly affect the properties of the perovskite. In this process, the temperature of heat treatment controls the particle size and the connectivity. The denser films are obtained at the lower temperatures

(650 °C). At higher temperature, the films are then formed of weakly connected grains of the perovskite phase, forming a 2-D conducting lattice near the percolation threshold. This will allow an investigation of the role of grain size and grain boundaries in the MR effect.

**Acknowledgment.** We thank F. Maroun for the SEM images and M. Morcrette and J. Perrière of the Groupe de Physique des Solides (Université Paris VI et VII) for the Rutherford backscattering spectrometry.

CM970664G